AD-A181 352 MILLIMETER-VISIBLE INJECTION LOCKING AND TESTING(U) 1/1
CALIFORNIA UNIV LOS ANGELES DEPT OF ELECTRICAL
ENGINEERING H FETTERMAN ET AL DEC 85 AFOSR-TR-87-0769
UNCLASSIFIED F49620-83-K-0016 F/G 9/1 NL

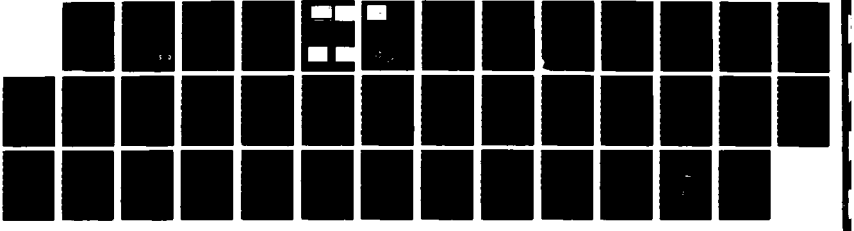

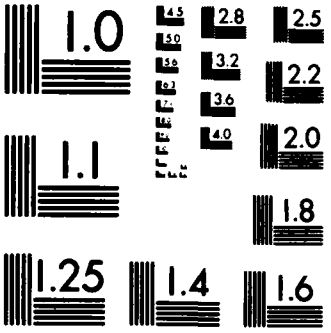

MICROCOPY RESOLUTION TEST CHART
NATIONAL BUREAU OF STANDARDS-1963-A

UNCLASSIFIED
IRITY CLASSIFICATION OF THIS

AD-A181 352 DTIC FILE COPY

REPORT DOCUMENTATION PAGE

1a. REPORT SECURITY CLASSIFICATION UNCLASSIFIED	1b. RESTRICTIVE MARKINGS
2a. SECURITY CLASSIFICATION AUTHORITY	3. DISTRIBUTION / AVAILABILITY OF REPORT Approved for Public Release; Distribution Unlimited
2b. DECLASSIFICATION / DOWNGRADING SCHEDULE	
4. PERFORMING ORGANIZATION REPORT NUMBER(S)	5. MONITORING ORGANIZATION REPORT NUMBER(S) AFOSR-TR- 87-0769
6a. NAME OF PERFORMING ORGANIZATION University of California 6b. OFFICE SYMBOL (If applicable)	7a. NAME OF MONITORING ORGANIZATION AFOSR/NP
6c. ADDRESS (City, State, and ZIP Code) Electrical Engineering Department Los Angeles, CA 90024	7b. ADDRESS (City, State, and ZIP Code) Building 410 Bolling AFB DC 20332-6448
8a. NAME OF FUNDING / SPONSORING ORGANIZATION Same as 7a 8b. OFFICE SYMBOL (If applicable)	9. PROCUREMENT INSTRUMENT IDENTIFICATION NUMBER F49620-83-K-0016
8c. ADDRESS (City, State, and ZIP Code) Same as 7b	10. SOURCE OF FUNDING NUMBERS PROGRAM ELEMENT NO. 61102F; PROJECT NO. 2301; TASK NO. A1; WORK UNIT ACCESSION NO.

11. TITLE (Include Security Classification)

"MILLIMETER-VISIBLE INJECTION LOCKING AND TESTING" (U)

12. PERSONAL AUTHOR(S)

Drs Harold Fetterman, Chewlan Liew, & Wai-Leung Ngai

13a. TYPE OF REPORT	13b. TIME COVERED	14. DATE OF REPORT (Year, Month, Day)	15. PAGE COUNT
FINAL	FROM 1 Jan 83 TO 31 Dec 85	Dec 85	37

16. SUPPLEMENTARY NOTATION

17. COSATI CODES			18. SUBJECT TERMS (Continue on reverse if necessary and identify by block number)
FIELD	GROUP	SUB-GROUP	
			Millimeter, Optical Mixing

19. ABSTRACT (Continue on reverse if necessary and identify by block number)

A visible-Millimeter Wave mixing system for testing high frequency devices has been set up with all components operating satisfactorily and locked to stabilized cavities. Using this system, mixing has been obtained, with frequency separations ranging to 100 GHz, in a number of GaAs and GaAs/AlGaAs devices. These devices include commercial FETs, state-of-the-art industrial FETs as well as modulation doped HEMT structures and Heterojunction bipolar transistors. Keywords: Field Effect Transistors, Gallium Arsenides; Aluminum Gallium Arsenide; High Electron Mobility Transistor;

DTIC
ELECTE
JUN 11 1987
S D
D

20. DISTRIBUTION / AVAILABILITY OF ABSTRACT ☒ UNCLASSIFIED/UNLIMITED ☒ SAME AS RPT. ☐ DTIC USERS	21. ABSTRACT SECURITY CLASSIFICATION Unclassified
22a. NAME OF RESPONSIBLE INDIVIDUAL Dr Howard R. Schlossberg	22b. TELEPHONE (Include Area Code) 202/767-4906 22c. OFFICE SYMBOL NP

DD FORM 1473, 84 MAR 83 APR edition may be used until exhausted. All other editions are obsolete.

SECURITY CLASSIFICATION OF THIS PAGE
UNCLASSIFIED

405206 CL

AFOSR-TR- 87-0769

FINAL REPORT

Approved for public release;
distribution unlimited.

TO

AIR FORCE OFFICE OF SCIENTIFIC RESEARCH

FOR

CONTRACT #F49620-83-K-0016

PERIOD OF PERFORMANCE: 1 JAN 83 - 31 DEC 85

FROM

THE UNIVERSITY OF CALIFORNIA

ELECTRICAL ENGINEERING DEPARTMENT

PRINCIPAL INVESTIGATOR: DR HAROLD FETTERMAN

AIR FORCE OFFICE OF SCIENTIFIC RESEARCH (AFSC)
NOTICE OF TRANSMITTAL TO DTIC
This technical report has been reviewed and is
approved for public release IAW AFR 190-12.
Distribution is unlimited.
MATTHEW J. KERPER
Chief, Technical Information Division

Accesion For
NTIS CRA&I ☒
DTIC TAB ☐
Unannounced ☐
Justification .....
By .....
Distribution /
Availability Codes
Dist | Avail and / or Special
A-1

QUALITY INSPECTED 1

Millimeter-Visible Injection Locking and Testing

Harold Fetterman, Chewlan Liew, and Wai-Leung Ngai
Electrical Engineering Department
University of California
Los Angeles
(213) 825-3431

Abstract

A Visible-Millimeter Wave mixing system for testing high frequency devices has been set up with all components operating satisfactorily and locked to stabilized cavities. Using this system, mixing has been obtained, with frequency separations ranging to 100 GHz, in a number of GaAs and GaAs/AlGaAs devices. These devices include commercial FETs, state of the art industrial FETs as well as modulation doped HEMT structures and Heterojunction bi-polar transistors.

Research Summary

It has been extremely difficult to make frequency response measurements of devices at millimeter wave frequencies. We have therefore implemented several optical techniques to identify and measure the millimeter wave performance of our newly developed modulation doped transistors. Of greatest versatility is our c.w. mixing approach which can test systems up to several hundred GHz. These experiments have been compared with results obtained using pulsed sources with good agreement.

Devices examined include commercial FETs, "state of the art" industrial FETs, HEMT structures fabricated as part of this program and newly developed high frequency Heterojunction bi-polar transistors. Many of the initial goals of this program have been achieved or are underway. Specifically:

1. Efficient mixing has been obtained in 0.5 and 0.25 micron commercial FETs at high frequencies. Injection locking has been demonstrated up to 20 GHz and is being extended to higher frequencies and bandwidths. Typical results at 5 GHz are indicated in Figure 1. The locking bandwidth seems to be limited to about 4 MHz and is under investigation.

2. Mixing in HEMT devices [1] has also been explored as a function of frequency and temperature. The improvement in transconductance and mobility as a function of temperature, shown in Figure 2, has been observed in the laser mixing efficiencies. New devices using the latest E-beam fabrication technology (0.20 micron gates) are now being developed and will be tested in this effort. These HEMT devices will be incorporated into hybrid oscillator circuits designed for operation at 90 GHz.

3. Tests have been made on a series of Heterojunction Bi-polar devices [2] using both mixing techniques and high speed pulsed semiconductor lasers. These experiments have confirmed the validity of the results from mixing experiments in the region of overlap. In addition, they have demonstrated that these heterojunciton devices are circuit limited and are capable of extremely high frequency behavior. Traces of the response of these devices using sampling scopes are shown in Figure 3. In Figure 4 we show the response obtained for the highest frequency transistors using mixing techniques. At this point the measurement is limited by the test fixture's parasitics.

Current efforts are to mount these devices into circuits as oscillators and amplifiers at millimeter wave frequencies. In order to accomplish this we have constructed a six port system to measure the relevant "S" parameters. Shown in Figure 5 is a diagram of this system now being used at 90 GHz. After identifying the high frequency devices using optical techniques, we find that we now can effectively design and construct three terminal oscillators for the millimeter.

References

1. C.Y. Chen, A.Y. Cho, C.G. Bethes, P.A. Garbinski, Y.M. Pang, B.F. Levine and K. Ogawa, App. Phys. Lett. 42 1040 (1983).
2. P.M. Asbeck, et al., "MM Wave Performance of GaAs/AlGaAs Heterojunction Bipolar Transistors (Proceedings IEDM, San Francisco 1984).

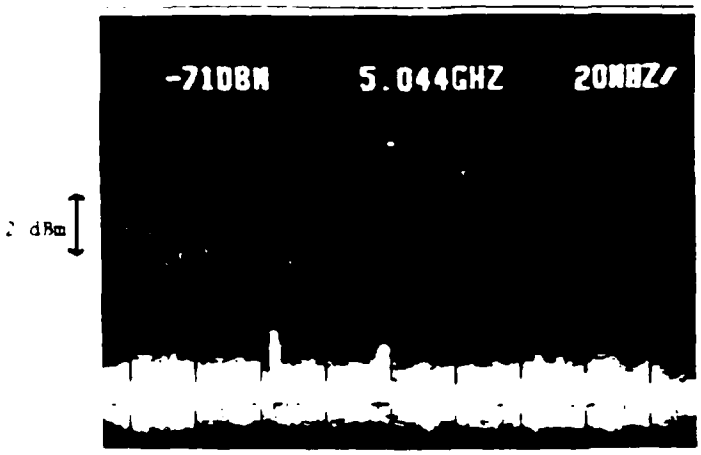

Figure 1b. Beat note approaches oscillator with f = 5.044 GHz.

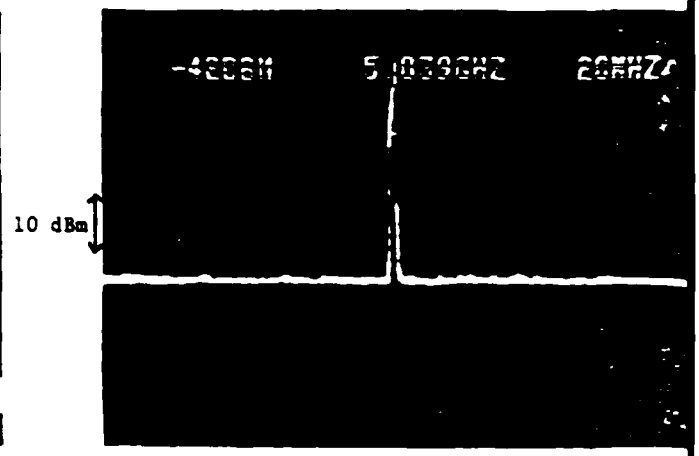

Figure 1b. Injection locking occurs with greatly increased power.

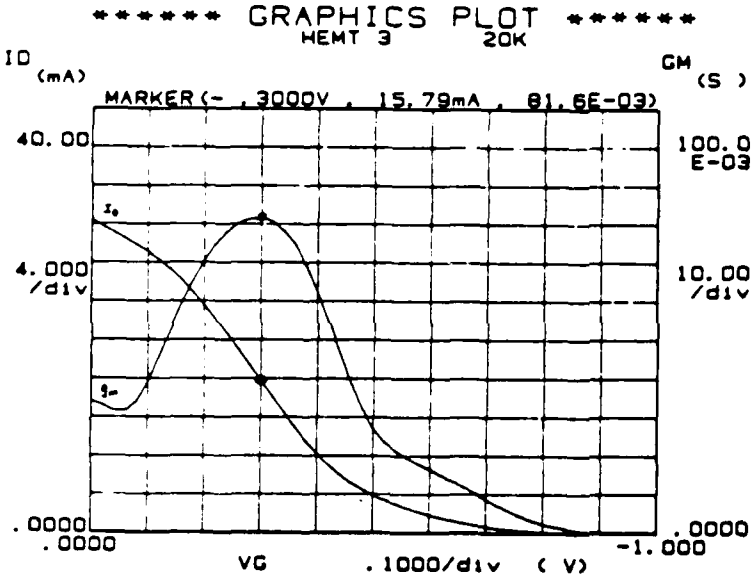

Figure 2. Transconductance at 20K showing the improvement in mobility of the GaAs 2D electron gas. This increase to over 260mS/mm is reflected in the optical mixing efficiency.

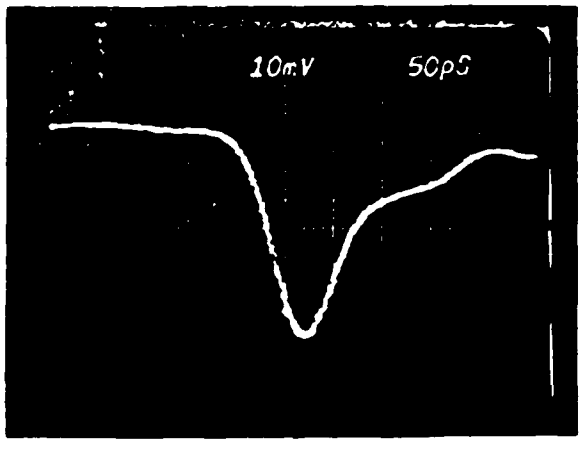

Figure 3a. Curve of semiconductor pulsed laser output using a fast photodiode showing a rise time of less than 50 ps. taken with a sampling scope.

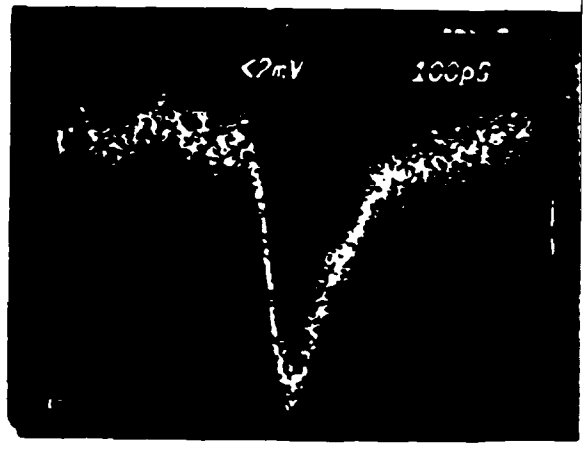

Figure 3b. Heterojunction Bi-polar's optical response. By injecting carriers directly into the base we are able to obtain intrinsic response measurements relatively independent of circuit parameters.

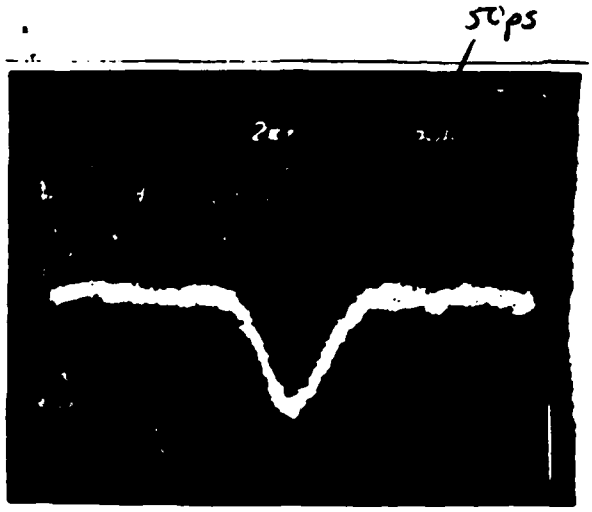

Figure 3c. The pulse response of a GaAlAs/GaAs FET tested using the laser diode.

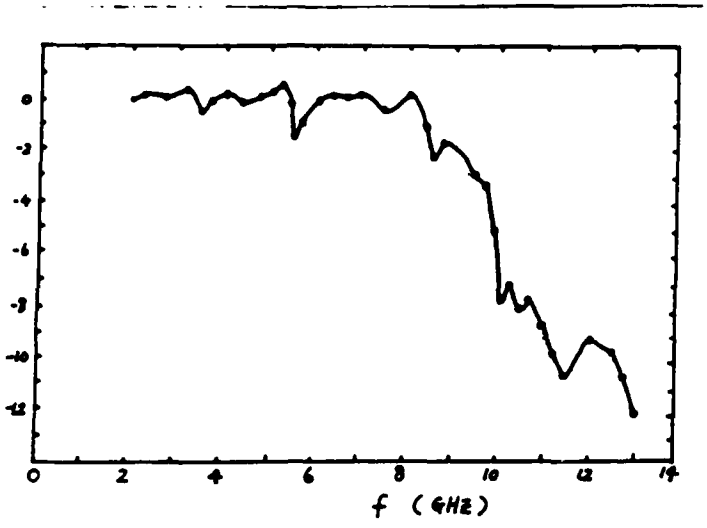

Figure 4. The frequency response measurement by the mixing experiment for the uniform band gap base transistor.

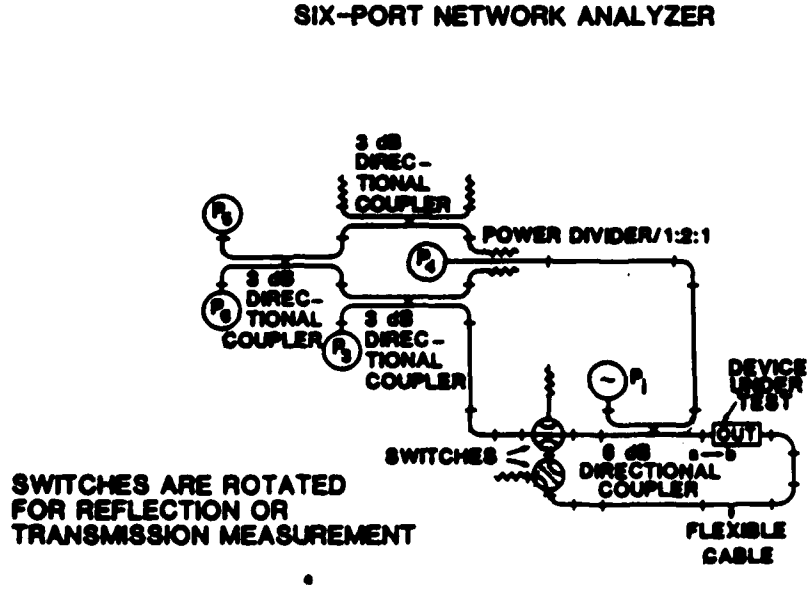

Figure 5. Six Port System to measure vector parameters at 90 GHz.

I. Introduction

In recent years the development of millimeter wave systems for missile guidance, radar, remote sensing, and communications has spurred advances in sources of millimeter waves. Traditional electronic tubes such as backward wave oscillators and klystrons are still used for high power applications [1]. In many millimeter wave systems such as airborne and satellite transmitters and receivers, space and weight are important design considerations. In such systems, solid state sources are preferred.

Today, two terminal solid state devices such as the IMPATT diode or the transferred-electron device (TED) provide power at millimeter wavelengths. IMPATT diodes can supply 2 W of continous wave power at 40 GHz and several mW at 230 GHz [2]. Transferred-electron devices can produce about 20 mW at 100 GHz [3]. These devices require distributed feedback for sustained oscillation, therefore they must be encapsulated in a waveguide cavity.

The development of microwave integrated circuits suggests the application of similar technology to millimeter wave integrated circuits. For these planar circuits, either field-effect transistors or bipolar transistors would be the active element. In particular, the gallium arsenide metal-semiconductor field-effect transistor (GaAs MESFET) has had the most success to date as a millimeter wave planar source. MESFET oscillators have recently been constructed to operate at 69 GHz [4] and 110 GHz [5]. The power produced by these devices has been on the order of 1 mW. Even though millimeter wave transistors are presently low power devices, they could be used in low

noise amplifiers, local oscillators, mixers, and active elements for imaging arrays.

Recently, another type of field-effect transistor, which is called the either the high electron mobility transistor (HEMT) or the modulation-doped field-effect transistor (MODFET), has shown promise as a high frequency device. The HEMT is a consequence of research conducted on heterojunction superlattices [6]. The heterojunction superlattice is an arrangement of alternating layers of gallium arsenide and aluminum gallium arsenide ($GaAs/Al_xGa_{1-x}As$). Each layer is typically 80 to 100 Å thick. The precise control needed to grow superlattice structures can be achieved with molecular-beam epitaxy. The $Al_xGa_{1-x}As$ layers are selectively doped with Si atoms, which are donors to $Al_xGa_{1-x}As$. The conduction band edge of GaAs is lower in energy than the donor states in the $Al_xGa_{1-x}As$ so that the free electrons from the $Al_xGa_{1-x}As$ layers move into the GaAs layers where they become confined. Since the mobile electrons are spatially separated from their parent doner atoms, ionized impurity scattering is significantly reduced. Thus, the electron mobility parallel to the heterojunction interfaces becomes enhanced, especially at low temperatures [7]. The highest reported low field electron mobiltiy that was obtained at low temperatures was 2×10^6 cm /V-sec [8].

Shubnikov-deHaas measurements on single $GaAs/Al_xGa_{1-x}As$ interfaces has shown that the free electrons form a two-dimensional electron gas (2DEG) in the GaAs at the interface [9]. The HEMT consists of a single $Al_xGa_{1-x}As/GaAs$ interface. A potential applied to a metal gate on top of the $Al_xGa_{1-x}As$ layer controls the charge density of the 2DEG thus modulating the current flow along the interface.

The first HEMT reported in the literature was fabricated by Mimura et. al. in 1980 [10]. Most of the research on HEMT's has been directed toward digital circuit applications. Here the HEMT has been shown to be superior in speed to the MESFET [8].

In the last few years, the microwave and millimeter wave properties of the HEMT have begun to be examined. Microwave HEMT's have been fabricated with gate lengths of 0.25 um [11],[12]. The small-signal equivalent circuits of these transistors were determined from measured scattering parameters. From these circuits, unity current gain cut-off frequencies of 47 GHz and 70 GHz were computed. Furthermore, theoretical calculations from a model HEMT has placed the unity current gain cut-off frequency as high as 92 GHz and the maximum frequency of oscillation at 191 GHz [13]. HEMT's have also been applied to oscillators at 44 GHz and amplifiers from 35 GHz to 40 GHz [14].

The goal of this research is to further the characterization of HEMT's at microwave and millimeter wave frequencies. At microwave frequencies, the scattering parameters of a HEMT will be measured as a function of temperature. It is expected that the performance of the transistor will improve when it is cooled to very low temperatures. The microwave measurement will utilize an automatic network analyzer. The millimeter wave scattering parameters will be measured using a six-port network analyzer that was constructed for W-band (75 GHz to 110 GHz). Finally, with the data obtained from these measurements, a HEMT millimeter wave oscillator will be designed and fabricated.

II. HEMT CONSTRUCTION

The HEMT consists of single GaAs/$Al_xGa_{1-x}As$ heterojunction. The $Al_xGa_{1-x}As$ layer is doped with Si to provide donor atoms with a concentration of about $10^{18} cm^{-3}$. A spacer layer of undoped $Al_xGa_{1-x}As$ which is 20 Å to 100 Å thick separates the GaAs and the n-type $Al_xGa_{1-x}As$. The undoped GaAs channel is grown on a semi-insulating of LEC substrate.

The electron affinity for GaAs is larger than that for $Al_xGa_{1-x}As$. As a result, a potential well is formed in the GaAs next to the $Al_xGa_{1-x}As$ layer, as shown in figure 1. Free electrons from the doped $Al_xGa_{1-x}As$ region fall into the sub-bands of the potential well. Since the potential well is narrow, the electrons form a two-dimensional electron gas (2DEG). The electron density of the 2DEG at equilibrium is

$$q n_s = D k T \log\left[\left(1 + e^{q(E_{F_0} - E_0)/kT}\right)\left(1 + e^{q(E_{F_0} - E_1)/kT}\right)\right]$$

where D is the two-dimensional density of states, E_{F_0} is the equilibrium Fermi level, and E_0 and E_1 are the first two sub-band energy levels [15].

The actual construction of a typical transistor is shown in figure 2. To understand the physical operation of the HEMT, the gradual channel approximation is used in the following explanation. When a negative potential is applied to the gate and a positive potential is applied to the drain, the 2DEG concentration varies as a function of gate voltage and the channel voltage as

$$Q_s(x) = q n_s(x) = \frac{\epsilon_2}{d_2}\left(V_G - V_C(x) - V_{OFF}\right)$$

where ϵ_2 is the dielectric constant of $Al_xGa_{1-x}As$, d_2 is the thickness of the $Al_xGa_{1-x}As$ layer and V_{off} is the turn-off voltage which is related to the material properties of the heterojunction and the device structure.

The current in the channel is

$$I = Q_s(x)\, Z\, v(x)$$

where Z is the gate width and v(x) is the electron velocity at x, the distance along the channel from the source. The electric fields along the channel can be large enough for the electron velocity to saturate at a critical field strength $\mathcal{E}_c$. If the electron velocity is approximated by

$$v = \begin{cases} \mu \mathcal{E} & \mathcal{E} < \mathcal{E}_c \\ v_s & \mathcal{E} \geq \mathcal{E}_c \end{cases}$$

with μ being the low field electron mobility and v_s the electron saturation velocity, then it can be shown that the saturation current for a short gate HEMT is given by

$$I_s = \frac{Z \epsilon_2 v_s}{d_2} \left(V_G - V_{off} - R_s I_s - \mathcal{E}_c L \right)$$

where L is the gate length and R_s is the source resistance. The transconductance is defined as

$$g_m = \frac{\partial I_D}{\partial V_G} = \frac{Z \epsilon_2 v_s}{d_2}$$

Since the electrons are physically removed from their donor ions, the

value of v_s should be that of intrinsic GaAs. The saturation velocity increases as the device is cooled because electron-phonon collisions decrease. Therefore, the transconductance should increase as the device is cooled. This is indeed what was observed on a 0.5 um gate length HEMT as shown in figures 3 and 4.

III. MICROWAVE MEASUREMENTS

A. Figures of Merit

The small-signal equivalent circuit of an FET is shown in figure 5 [16]. The relationship of the lumped model components to the physical HEMT structure is shown in figure 6. The small-signal model is used to calculate various figures of merit of the transistor. Of particular importance is the transistor's stability, maximum available gain, and the maximum frequency of oscillation [17],[18],[19]. These quantities may be calculated by considering the transistor as a two-port circuit with the source terminal grounded, the gate terminal as the input , and the drain terminal as the output. From the equivalent circuit, the admittance parameters, which relate the input and output currents to the input and output voltages, can be determined. Also, the scattering parpameters can be derived from the admittance parameters, and vice versa. These relationships are shown in figure 7.

The internal feedback of the transistor may cause it to oscillate even is the absence of external feedback. A stability factor k is given by

$$k = \frac{2\,\mathrm{Re}\,y_{11}\cdot \mathrm{Re}\,y_{22} - \mathrm{Re}(y_{12}y_{21})}{|y_{12}|\,|y_{21}|}$$

When the stability factor is greater than one, the transistor is unconditionally stable. This means that the transistor will not suffer internal oscillations regardless of the source or load admittance. If k is between -1 and 1, the transistor is conditionally stable. In this case stability may be acheived under some source and load admittances.

When the transistor is unconditionally stable, the maximum available gain (MAG) is calculated from

$$MAG = \left|\frac{y_{21}}{y_{12}}\right| \frac{1}{K + \sqrt{K^2 - 1}}$$

The MAG is the power gain of the transistor when the source and load terminations are conjugates to the two-port input and output admittances, respectively. If the transistor is conditionally stable, the unilateral gain (U) is the maximum available gain of the device when an external feedback circuit has eliminated y_{12} . It is given by

$$U = \frac{|y_{21} - y_{12}|^2}{4\left(\mathrm{Re}\,y_{11}\cdot \mathrm{Re}\,y_{22} - \mathrm{Re}\,y_{12}\cdot \mathrm{Re}\,y_{21}\right)}$$

MAG and U have unity gain at the maximum frequencies of oscillation f_{max} and f_u .

B. Experiment

The two-port scattering parameters of a 0.25 um gate length HEMT that

was fabricated by TRW were measured. The transistor was mounted on a chip carrier and wire bonded to 50Ω microstrip transmission lines. Flange mount jack receptacles (Omni Spectra #2052-5636-02) were silver epoxied to the microstrip lines to provide transitions to SMA type connectors. The chip carrier was fastened to a copper cold finger that was located in a gas helium refrigerator. A Hewlett-Packard 8510 Automatic Network Analyzer was used to measure the scattering parameters of the HEMT from 2 GHz to 15 GHz. The temperature of the transistor was varied from 297 K to 20 K.

The small-signal equivalent circuit of the transistor was calculated from the scattering parameter values over the frequency range by using the optimization routines available on Super-Compact®, the microwave circuit analysis program [20]. The HEMT gate bias voltage, for a given drain voltage, was located at the point of maximum transconductance as determined from the DC current-voltage curves obtained by a semiconductor parameter analyzer. Figure 8 shows the small-signal equivalent circuits of the HEMT at 297 K and 20 K. The maximum frequencies of oscillation increased from 75 GHz to 87 GHz as the transistor was cooled. It should also be noted that the transconductance increased from 20 mS to 27 mS.

IV. MILLIMETER WAVE MEASUREMENTS

A. Six-Port Network Analyzer

The microwave measurements indicate that the 0.25 um gate length HEMT is capable of providing gain up into W-band frequencies. However, to understand the device operating characteristecs at these frequencies it it necessary to measure the scattering parameters of the HEMT directly. To accomplish this task, a W-band six-port network analyzer [21] has been constructed.

The general six-port junction is shown in figure 9. Since the six-port junction is linear, the waves travelling away from the junction can be related to the waves travelling toward the junction by 36 scattering parameters. The outgoing wave at the ith port can be written as

$$b_i = \sum_{j=1}^{6} S_{ij}\, a_j \qquad i = 1, \ldots, 6$$

where a_j is the incoming wave at the jth port and S_{ij} is the scattering parameter that relates the wave coming out of port i to an input wave at port j when all other ports are match terminated. Power meters are attached to four of the six ports. Each power meter presents a reflection coefficient to the junction port with which it is connected, so that

$$a_j = b_j \Gamma_j^{\rho} \qquad j = 3, \ldots, 6$$

Thus, there exists ten equations describing the six-port and twelve unknowns (a_i, b_i). The system of equations may be solved for ten of the variables in terms of the two remaining varialbles as

$$b_i = A_i a_2 + B_i b_2 \qquad i = 3, \ldots, 6$$

where A_i and B_i are functions of the S_{ij}'s and the Γ_i^{ρ}'s.

The power measured at the ith port is given by

$$P_i = |b_i|^2 = |A_i|^2 |a_2|^2 + A_i B_i^* b_2 a_2^* + A_i^* B_i b_2^* a_2 + |B_i|^2 |b_2|^2 \qquad i = 3, \ldots, 6$$

The quantities $|b_2|^2$, $b_2 a_2^*$, $b_2^* a_2$, and $|a_2|^2$ may be solved in terms of the measured powers P_i. If an unknown load is placed on port 2 with the signal source located at port 1, then

$$\Gamma_l = \frac{a_2}{b_2} = \frac{b_2^* a_2}{|b_2|^2} = \frac{\sum_{i=3}^{6} (x_i + j y_i) P_i}{\sum_{i=3}^{6} \rho_i P_i}$$

where x_i, y_i, and ρ_i are functions of all A_i and B_i. In practice, x_i, y_i, and ρ_i are determined by calibration where known loads are placed on port 2 and the measured powers are recorded.

For operation at W-band, the six-port network analyzer was constructed from WR-10 waveguide components. A schematic of the system is shown in figure 10. Two waveguide switches enable the six-port network analyzer to measure transmission coefficients as well as reflection coefficients. The calibration of the six-port can be done with four offset short circuits as the load standards [22]. The six-port is currently being programmed for data recording, calibration, and measurement.

B. HEMT Scattering Parameter Measurement

To measure the W-band scattering parameters of the HEMT, it is necessary to build waveguide to microstrip transitions. A ridged waveguide transition was chosen for optimum bandwidth. The transition was designed to produce a Chebyshev impedance transformation from WR-10 waveguide (cross-section 0.1" x 0.05") to 50 microstrip transmission lines [23], [24]. A drawing of the transition is shown in figure 11. A test fixture consisting of two transitions separated by a length of microstrip line between then has been constructed. The microstrip lines are 0.011" wide and were fabricated on 0.005" thick quartz substrates [25]. Small microstrip loads were machined from waveguide absorber (Eccosorb MF117). The return loss of a transition was measured and it is shown in figure 12. It indicates an average return loss of better than 15 dB across the band.

For millimeter wave characterization, the HEMT will be centered in the test fixture between the two transitions. The gate and drain will be bonded to the microstrip lines. DC voltage will be applied through a bias circuit. The six-port will be calibrated in waveguide. Next the test fixture including transitions and the HEMT will be tested. Then, by measuring the return loss of the transition and the insertion loss of the test fixture with a straight through length of microstrip line, the scattering parameters of the HEMT can be de-embedded from the measured scattering parameters.

IV. MILLIMETER WAVE HEMT OSCILLATOR

A prototype 94 GHz HEMT oscillator was designed and fabricated. Since no HEMT microwave data was available, a small-signal equivalent circuit of a microwave 0.25 um gate length GaAs MESFET was supplied by Hughes Aircraft Co. Research Laboratory. The model was derived from measured S-parameters up to 26 GHz. It was felt that the high frequency MESFET would be similar in operation to a high frequency HEMT, so that the design of a protype oscillator was attempted.

The oscillator circuit was designed using Super-Compact®. An impedance on the drain and the source terminals of the transistor was varied until the maximum negative resistance obtainable at the gate terminal was found. Then, the reactance at the gate was tuned out by placing a conjugate reactance at the gate. As figure 13 shows, inductances were required at all terminals of the transistor. A negative input resistance of -18Ω at 94 GHz was then available at the gate when the drain terminal load resistance was 200Ω.

The circuit realization is shown in figure 14. All circuit components were fabricated on 0.005" fused silica substrates using a gold up-plating process. The inductances were realized by open circuited microstrip stubs. The circuit pieces were bonded around a TRW 0.25 um gate length HEMT.

Since the circuit was to be placed inside the vacuum jacket of the gas helium refrigerator, an electromagnetically coupled dipole antenna was used as the output load [26]. A signal generated by the oscillator would then be radiated out through a window to a detector outside the vacuum jacket. A model

of the dipole was tested between 6 GHz and 9 GHz to determine the proper length and position from the feed point to provide a 50Ω match. The model was then scaled down so that the dipole would be resonant at 94 GHz. The antenna dimensions are shown in figure 14.

Upon testing the oscillator, no signal was observed at room temperature. However, at 50 K a 35 GHz signal was detected. Altering the circuit external to the transistor did not change theis oscillation frequency. It was concluded that the oscillation was due to the transistor's internal feedback. It may be possible to eliminate this unwanted oscillation through the use of a proper size chip capacitor in the bias line to provide a 35 GHz ground.

The prototype oscillator suffered two major drawbacks. One was the inability to experimentally tune the oscillator. The other was the use of the electromagnetically coupled dipole which at these frequencies is too small to successfully find the location from the feedpoint for an impedance match. Figure 15 is a sketch of an improved HEMT oscillator design. Tuning is accomplished by using bond wires or ribbons between small gold patches as a means of altering the length of the microstrip stubs. Then, instead of the electromagnetically coupled dipole at the output, a microstrip transition to a 50Ω line is inserted so that the waveguide to microstrip transition can be incorporated in the design. Of course, the final design would depend on the measured scattering parameters of the HEMT.

VI. CONCLUSION - FUTURE WORK

The microwave measurements on the 0.25 um gate length HEMT have indicated its ability to provide gain at millimeter wave frequencies. Refined microwave measurements are planned. Recently, a new SMA to microstrip connector (Wiltron K connector) that has a 15 dB or greater return loss up to 40 GHz has become commercially available. Therefore, it is planned to have a new microwave test fixture fabricated with these new connectors. Also, the test fixture will be made long enough to enable the use of time domain reflectometry (TDR) which is built in to the Automatic Network Analyzer. TDR allows one to record the frequency response of a device and test fixture, then to window out the test fixture connectors in the time domain, and finally to convert back into the frequency domain to obtain the response of the device alone.

When the six-port network analyzer is finally programmed to calibrate and measure reflection and transmission coefficients, its operation will be verified by inserting a load consisting of a variable phase shifter and a variable attenuator. The accuracy of the attenuator is specified to be within 0.1 dB, and the accuracy of the phase shifter is specified to be within 4°.

After the six-port network analyzer operation is verified, the scattering parameters of the 0.25 um gate length HEMT can be measured. A new waveguide to microstrip test fixture must be built to assure the critical alignment of the HEMT with the microstrip and the microstrip with the ridged waveguide of the transitions.

Finally, a millimeter wave HEMT oscillator will be designed using the

measured scattering parameters. If the HEMT is characterized at a few frequencies within the W-band then the small-signal equivalent circuit of the millimeter wave HEMT can be obtained. This would then be the transistor model used to optimize the oscillator circuit design.

The advances in microwave and millimeter wave electronics that would be obtained from this research project is summarized in the following list:

1. The HEMT will be characterized at microwave frequencies as a function of temperature.
2. The HEMT will be evaluated at millimeter wavelengths (W-band).
3. Scattering parameters of an active device will be made using a six-port network analyzer.
4. A millimeter wave HEMT oscillator will be designed from measured W-band scattering parameters.

The conclusions drawn from this work should define and stimulate future research on the HEMT as a millimeter wave circuit element.

VII. REFERENCES

1. J. C. Wiltse, "Introduction and Overview of Millimeter Waves", Infrared and Millimeter Waves, Vol. 4, Kenneth J. Button and James C. Wiltse eds., Academic Press, New York, 1981.

2. H. J. Kuno, "IMPATT Devices for Generation of Millimeter Waves", Infrared and Millimeter Waves, Vol. 1, Kenneth J. Button ed., Academic Press, New York, 1979.

3. I. G. Eddison, "Indium Phoshide and Gallium Arsenide Transferred-Electron Devices", Infrared and Millimeter Waves, Vol. 11, Kenneth J. Button ed., Academic Press, New York, 1984.

4. D. W. Maki, J. M. Schellenberg, H. Yamasaki, L. C. T. Liu, "A 69 GHz Monolithic FET Oscillator", IEEE 1984 Microwave and Millimeter Wave Monolithic Circuits Symposium Digest, pp. 62-66.

5. H. Q. Tserng, B. Kim, "110 GHz GaAs FET Oscillator", Electronic Letters, Vol. 21, No. 5, p. 178, February 28, 1985.

6. L. Esaki, R. Tsu, "Superlattice and Negative Differential Conductivity in Semiconductors", IBM J. Res. Develop., pp. 61-61, January 1970.

7. R. Dingle, H. L. Störmer, A. C. Gossard, W. Wiegmann, "Electron Mobilities in Modulation-Doped Semiconductor Heterojuction Superlattices", Appl. Phys. Lett., Vol. 33, p. 665, 1978.

8. P. M. Soloman and H. Morkoç, "Modulation-Doped GaAs/AlGaAs Heterojunction Field-Effect Transistors (MODFET's), Ultrahigh-Speed Device for Supercomputers", IEEE Trans. Electron Devices, Vol. ED-31, No. 8, August 1984.

9. H. L. Störmer, R. Dingle, A. C. Gossard, W. Wiegmann, M. D. Sturge, "Two-Dimensional Electron Gas At a Semiconductor-Semiconductor Interface", Solid State Communications, Vol. 29, pp. 705-709, 1979.

10. T. Mimura, S. Hiyamizu, T. Fujii, K. Nanbu, "A New Field-Effect Transistor with Selectively Doped GaAs/n-$Al_xGa_{1-x}As$ Heterojunctions", Japanese Journal of Applied Physics, Vol. 19, No. 5, pp. L225-L227, May 1980.

11. J. J. Berenz, K. Nakano, K. P. Weller, "Low Noise High Electron Mobility Transistors", IEEE 1984 Microwave and Millimeter-Wave Monolithic Circuits Symposium Digest.

12. U. K. Mishra, S. C. Palmateer, P. C. Chao, P. M. Smith, J. C. M. Hwang, "Microwave Performance of 0.25-um Gate Length High Electron Mobility Transistors", IEEE Electron Device Letters, Vol. EDL-6, No. 3, March 1985.

13. M. B. Das, "A High Aspect Ratio Design Approach to Millimeter-Wave HEMT Structures", IEEE Trans. Electron Devices, Vol. ED-31, No. 1, January 1985.

14. M. Sholley, S Maas, B. Allen, R. Savires, A. Nichols, J. Abell, "HEMT mm-Wave Amplifiers, Mixers, and Oscillator", Microwave Journal, Vol. 28, No. 8, pp. 121-131, August 1985.

15. D. Delagebeaudeuf, N. T. Linh, "Metal-(n) AlGaAs-GaAs Two-Dimensional Electron Gas FET", IEEE Trans. Electron Devices, Vol. ED-29, No. 6, pp. 955-960, June 1982.

16. D. J. Arnold, R. Fischer, W. F. Kopp, T. S. Henderson, H. Morkoc, "Microwave Characterization of (Al,Ga)As/GaAs Modulation-Doped FET's: Bias Dependence of Small-Signal Parameters", IEEE Trans. Electron Devices, Vol. ED-31, No. 10, pp. 1399-1402, Oct. 1984.

17. J. M. Rollett, "Stability and Power-Gain Invariants of Linear Twoports", IRE Trans. Circuit Theory, Vol. CT-9, No. 29, March 1962.

18. A. P. Stern, "Stability and Power Gain of Tuned Transistor Amplifiers", Proc. IRE, Vol. 45, pp. 271-283, March 1957.

19. P. Wolf, "Microwave Porperties of Schottky-barrier Field-Effect Transistors", IBM J. Res. Develop., pp. 125-141, March 1970.

20. Super-Compact®, Comsat General Integrated Systems, Inc., Version 1.6.

21. G. F. Engen, "The Six-Port Reflectometer: An Alternative Network Analyzer", IEEE Trans. Microwave Theory Tech., Vol. MTT-25, pp. 1075-1080, December 1977.

22. S. Li, R. G. Bosisio, "Calibration of Multiport Reflectometers by Means of Four Open/Short Circuits", IEEE Trans. Microwave Theory Tech., Vol. MTT-30, No. 7, pp. 1085-1090, July 1982.

23. S. B. Cohn, "Optimum Design of Stepped Transmission Line Transformers", IRE Trans. Microwave Theory Tech., pp. 16-21, April 1955.

24. W. J. R. Hoefer, N. N. Burton, "Closed-Form Expression for the Parameters of Finned and Ridged Waveguides", IEEE Trans. Microwave Theory and Tech., Vol. MTT-30, No. 12, pp. 2190-2194, December 1982.

25. K. Chang, F. Hsu, J. Berenz, K. Nakano, "Find Optimum Substrate Thickness for Millimeter Wave GaAs MMICs", Microwaves and RF, pp. 123-128, September 1984.

26. H. G. Oltman, "Electomagnetically Coupled Microstrip Dipole Antenna Elements", Proc. 8th European Microwave Conference, Paris, France, September 1978.

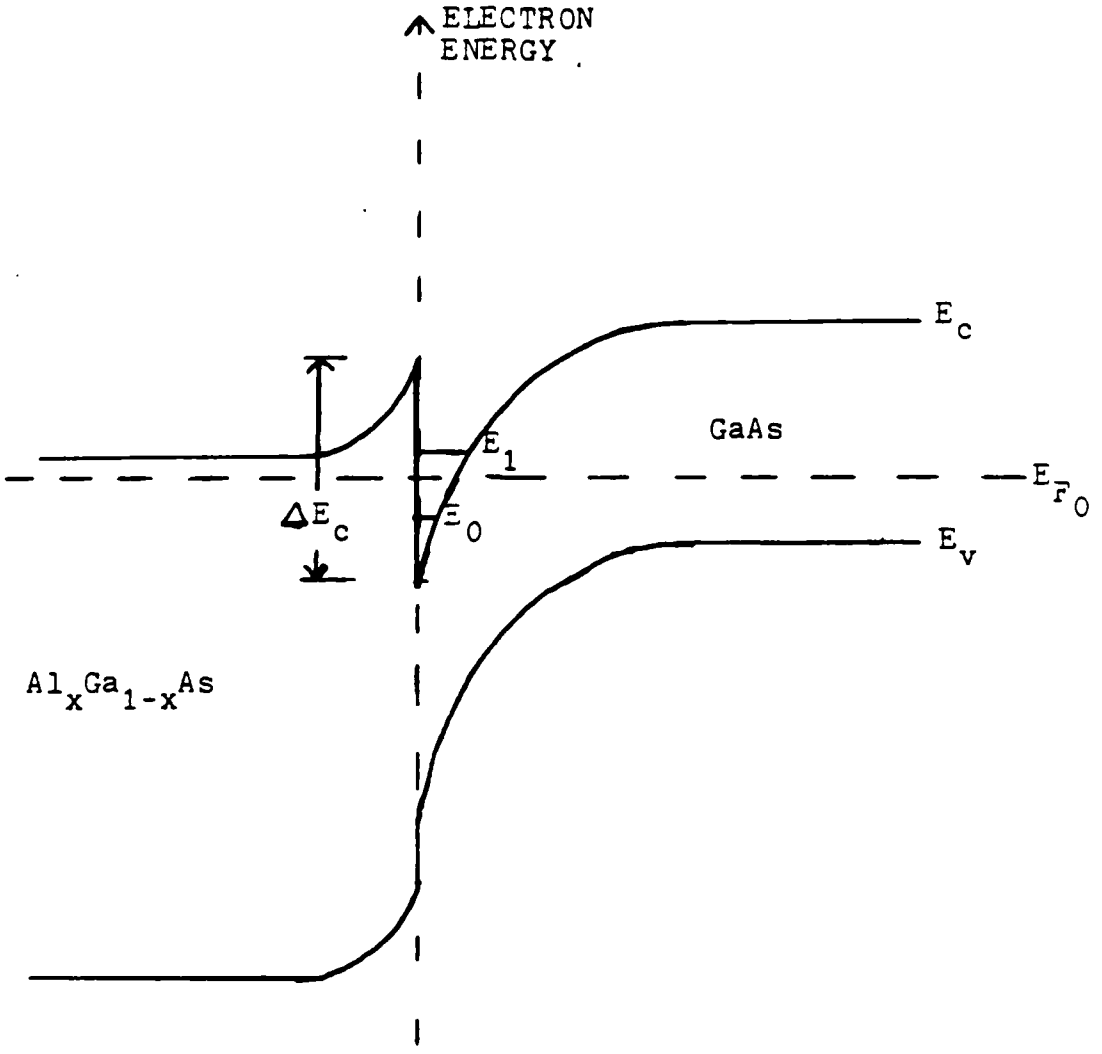

Figure 1. $Al_xGa_{1-x}As/GaAs$ Heterojunction at Equilibrium

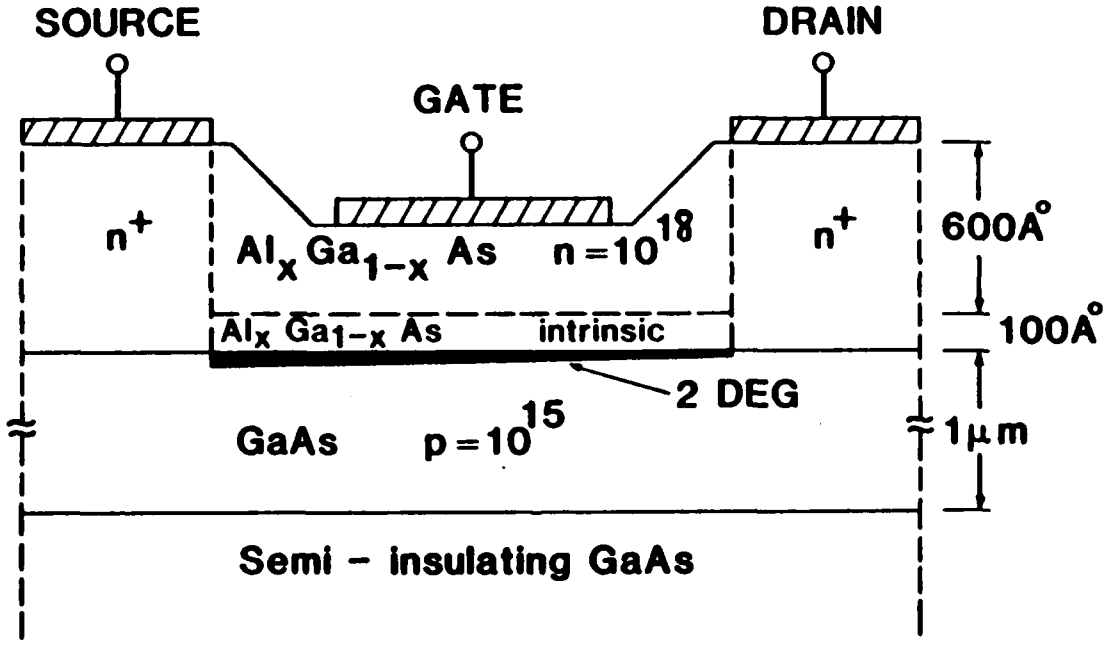

Figure 2. Typical HEMT Cross Section

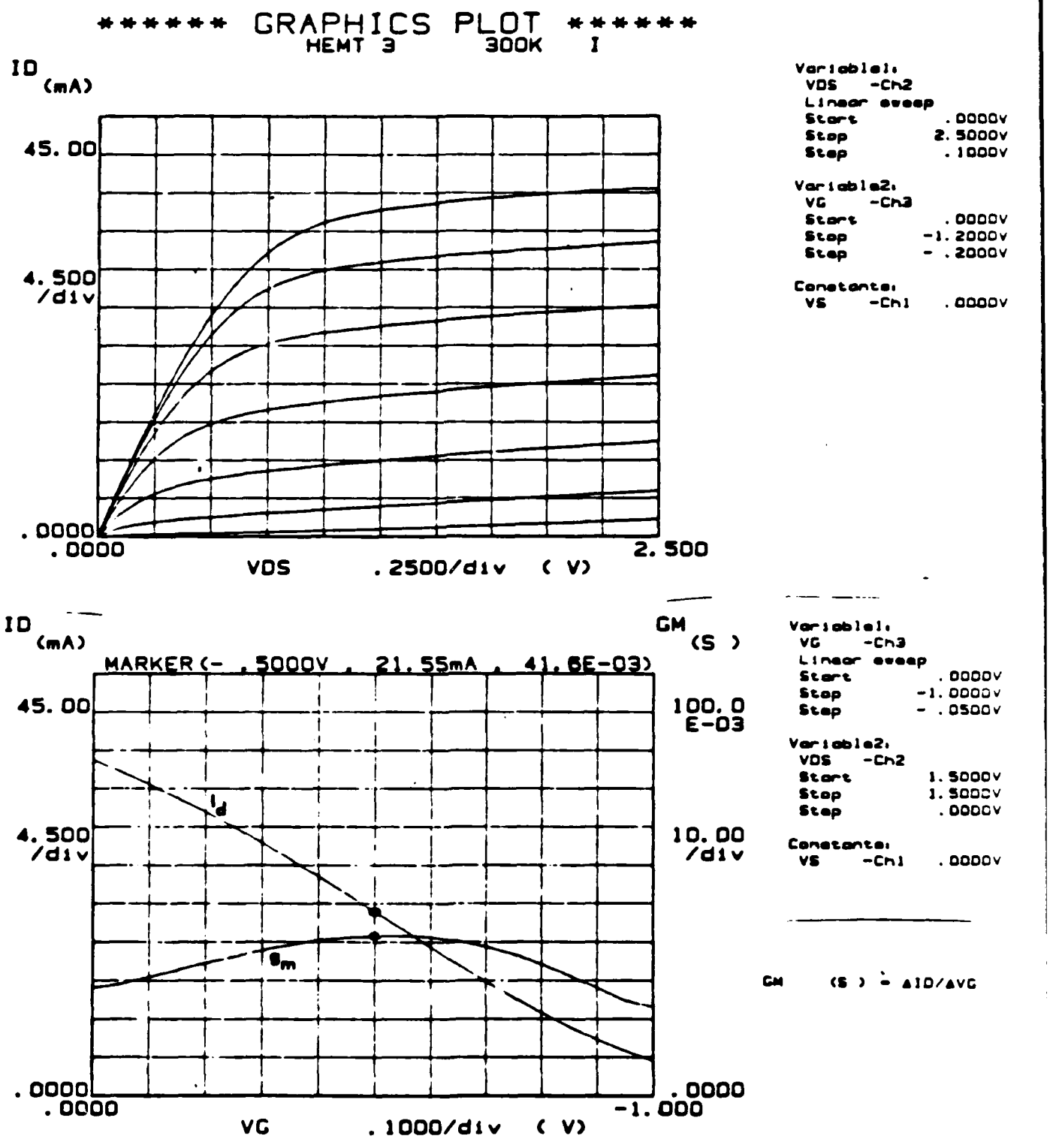

Figure 3. 0.5 um Gate Length HEMT - 300 K

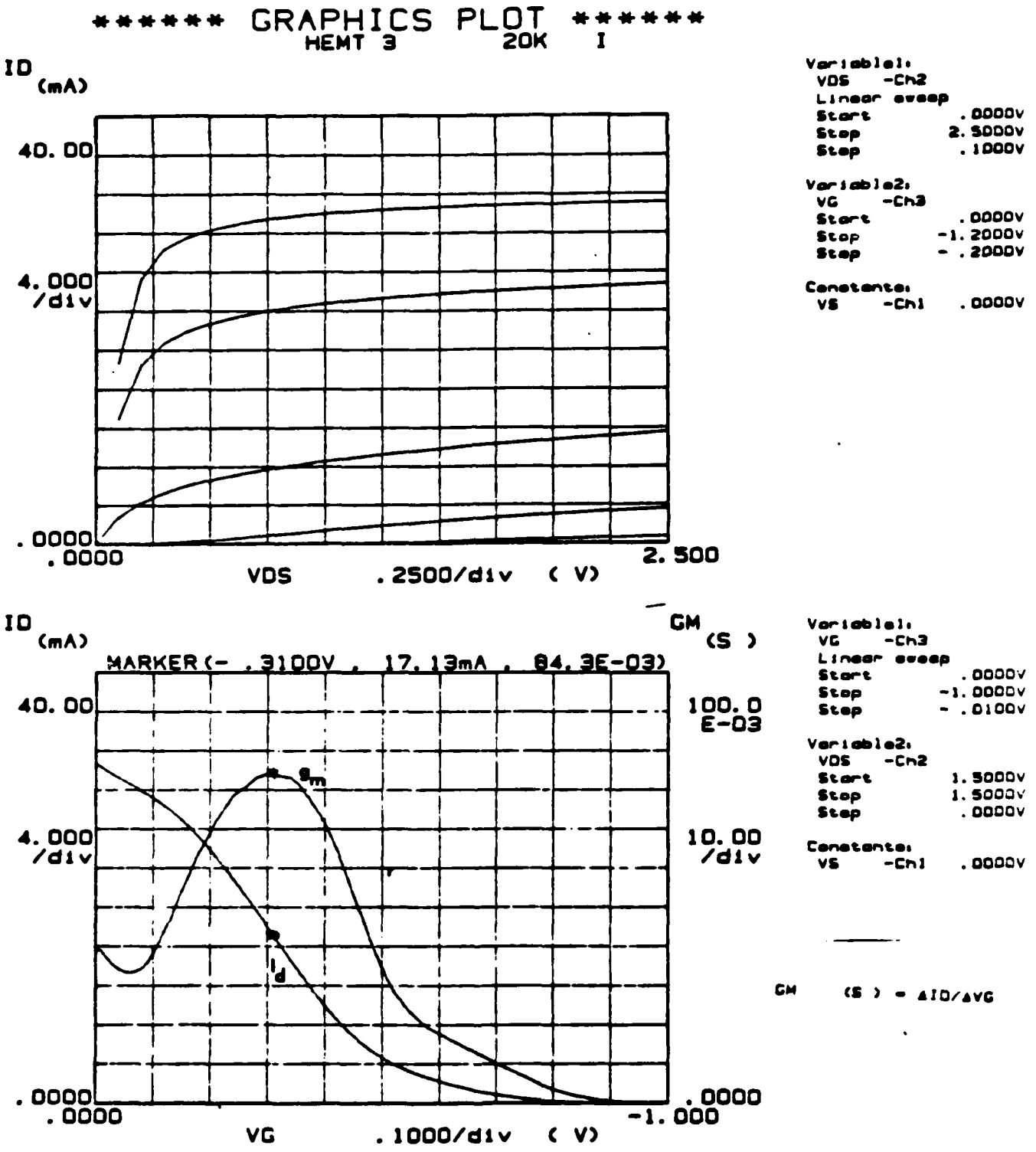

Figure 4. 0.5 um Gate Length HEMT - 20 K

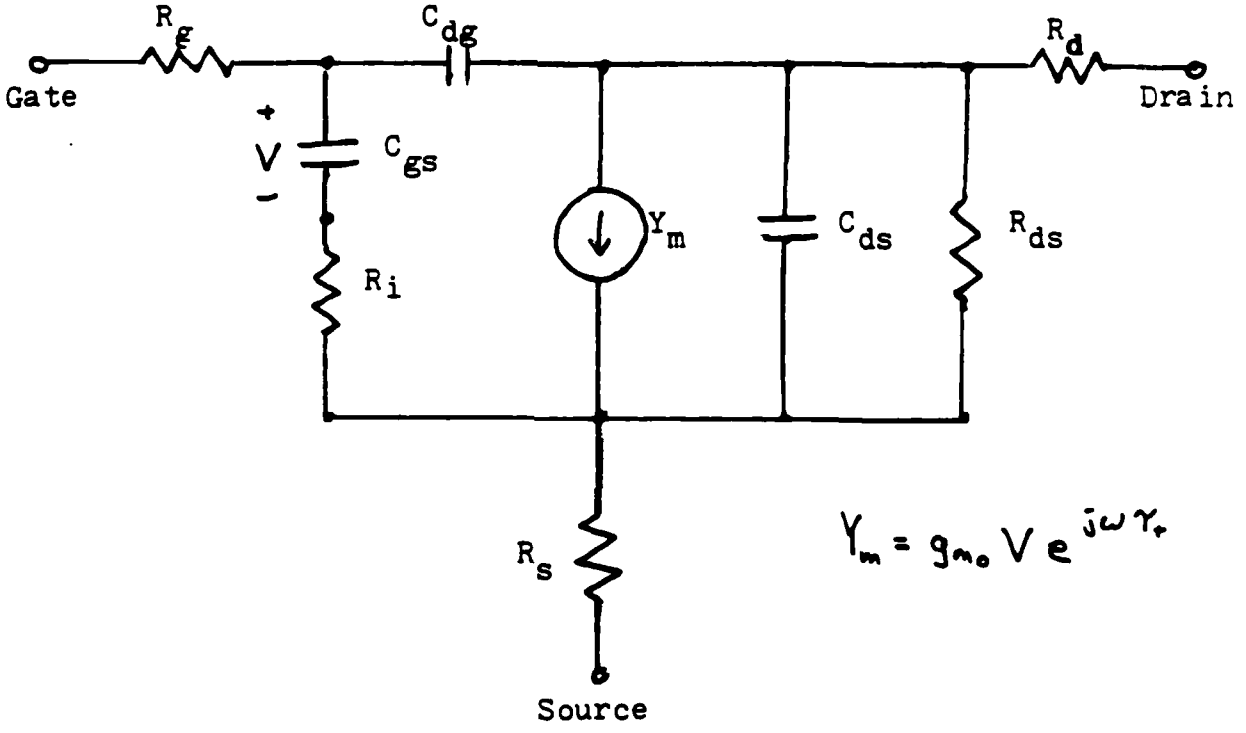

Figure 5. Small-Signal Equivalent Circuit

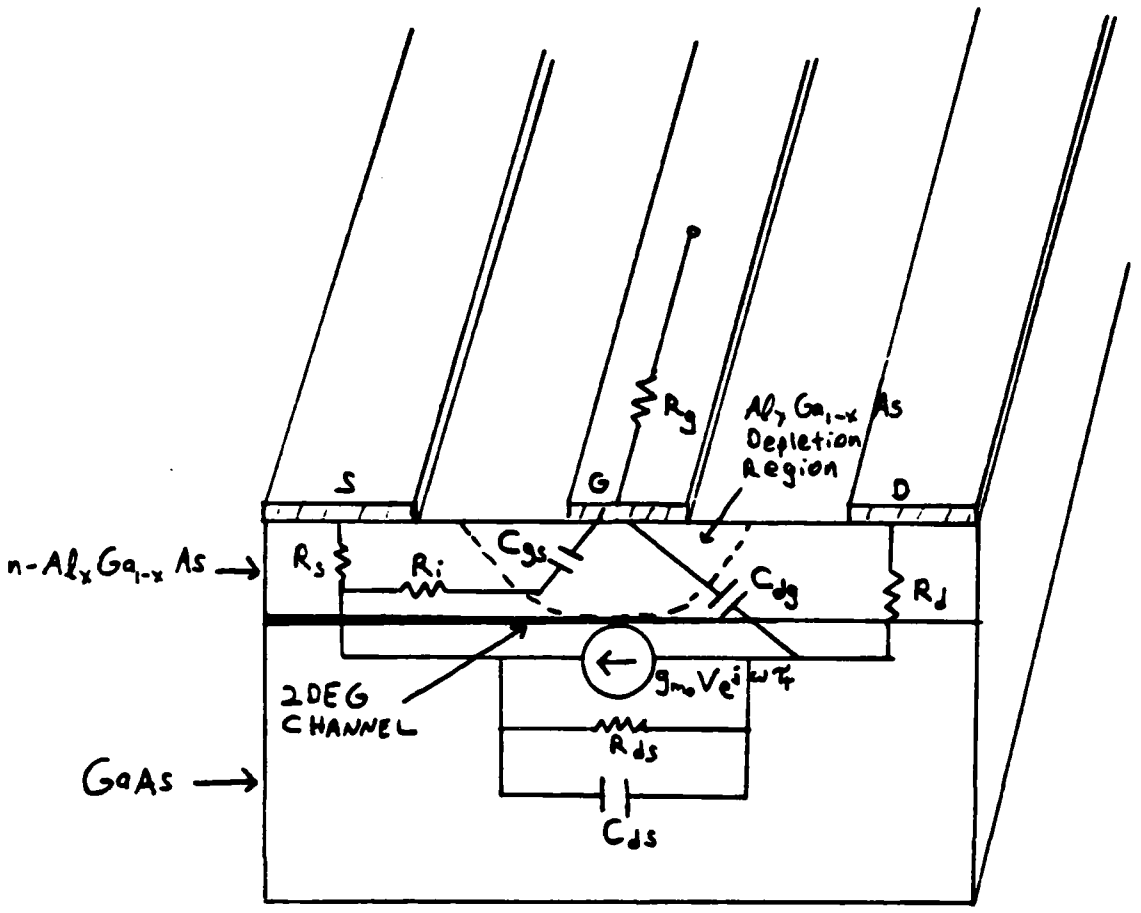

g_{m_0} - transconductance

R_{ds} - channel output resistance

C_{ds} - channel dipole layer capacitance

C_{gs} - gate-to-source capacitance

C_{dg} - gate-to-drain feedback capacitance

R_i - channel input resistance

R_g - gate metallization resistance

R_s, R_d - source and drain contact resistance and bulk resistance

τ_+ - channel phase delay

Figure 6. Physical HEMT Model

$$I_1 = y_{11}V_1 + y_{12}V_2$$

$$I_2 = y_{21}V_2 + y_{22}V_2$$

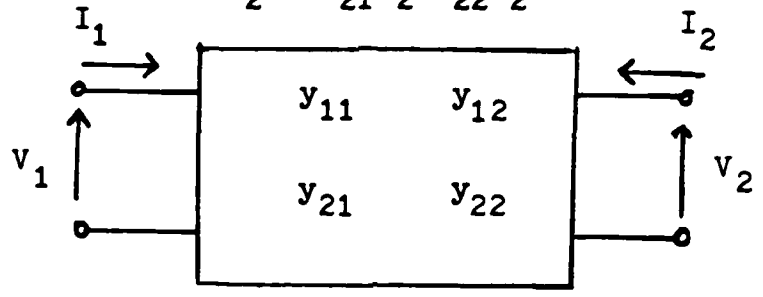

a) Admittance Parameters

$$b_1 = S_{11}a_1 + S_{12}a_2$$

$$b_2 = S_{21}a_1 + S_{22}a_2$$

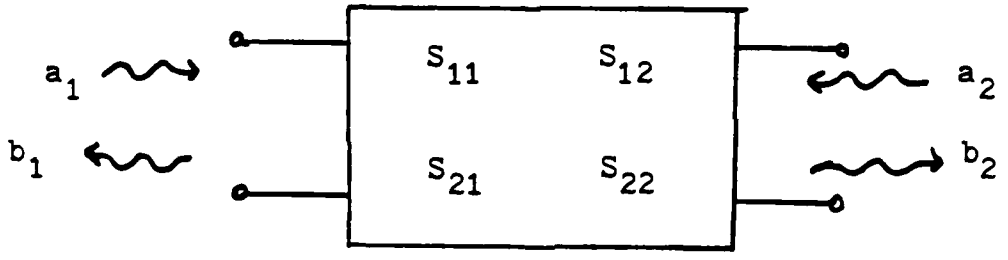

b) Scattering Parameters

$$y_{11} = \frac{S_{12}S_{21} + (1-S_{11})(1+S_{22})}{-S_{12}S_{21} + (1+S_{11})(1+S_{22})} \cdot \frac{1}{Z_0}$$

$$y_{12} = \frac{-2S_{12}}{-S_{12}S_{21} + (1+S_{11})(1+S_{22})} \cdot \frac{1}{Z_0}$$

$$y_{21} = \frac{-2S_{21}}{-S_{12}S_{21} + (1+S_{11})(1+S_{22})} \cdot \frac{1}{Z_0}$$

$$y_{22} = \frac{S_{12}S_{21} + (1+S_{11})(1-S_{22})}{-S_{12}S_{21} + (1+S_{11})(1+S_{22})} \cdot \frac{1}{Z_0}$$

Figure 7. Two-Port Admittance and Scattering Parameters

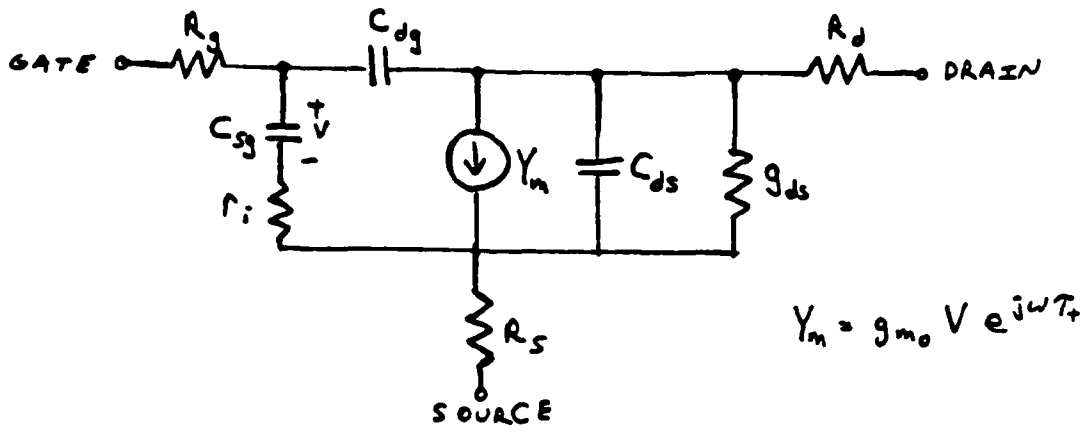

	297 K	20 K
V_{ds}	2.5V	2.5 V
V_g	-0.05V	-0.15 V
g_{m0}	0.02033 S	0.02765 S
C_{sg}	0.164 pS	0.185 pF
τ_t	1.82×10^{-12} sec	12.1×10^{-12} sec
C_{dg}	460 pF	1.5×10^{-3} pF
g_{ds}	1.95×10^{-3} S	2.0×10^{-3} S
r_i	1.558	0.441
r_g	0.0431	0.0925
r_d	0.6374	0.211
r_s	7.104	8.61
C_{ds}	2.31 pF	0.0164 pF
f_t	20 GHz	23.7 GHz
f_u	75.2 GHz	87.7 GHz

Figure 8. HEMT Equivalent Circuits at 297 K and 20 K

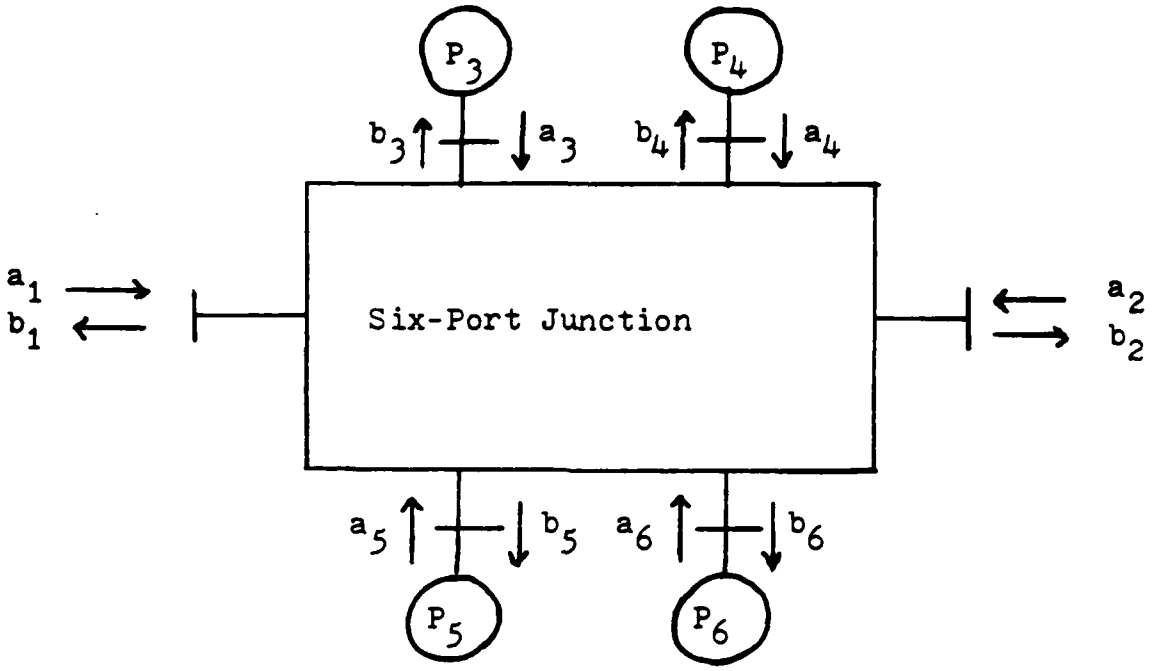

Figure 9. General Six-Port Junction

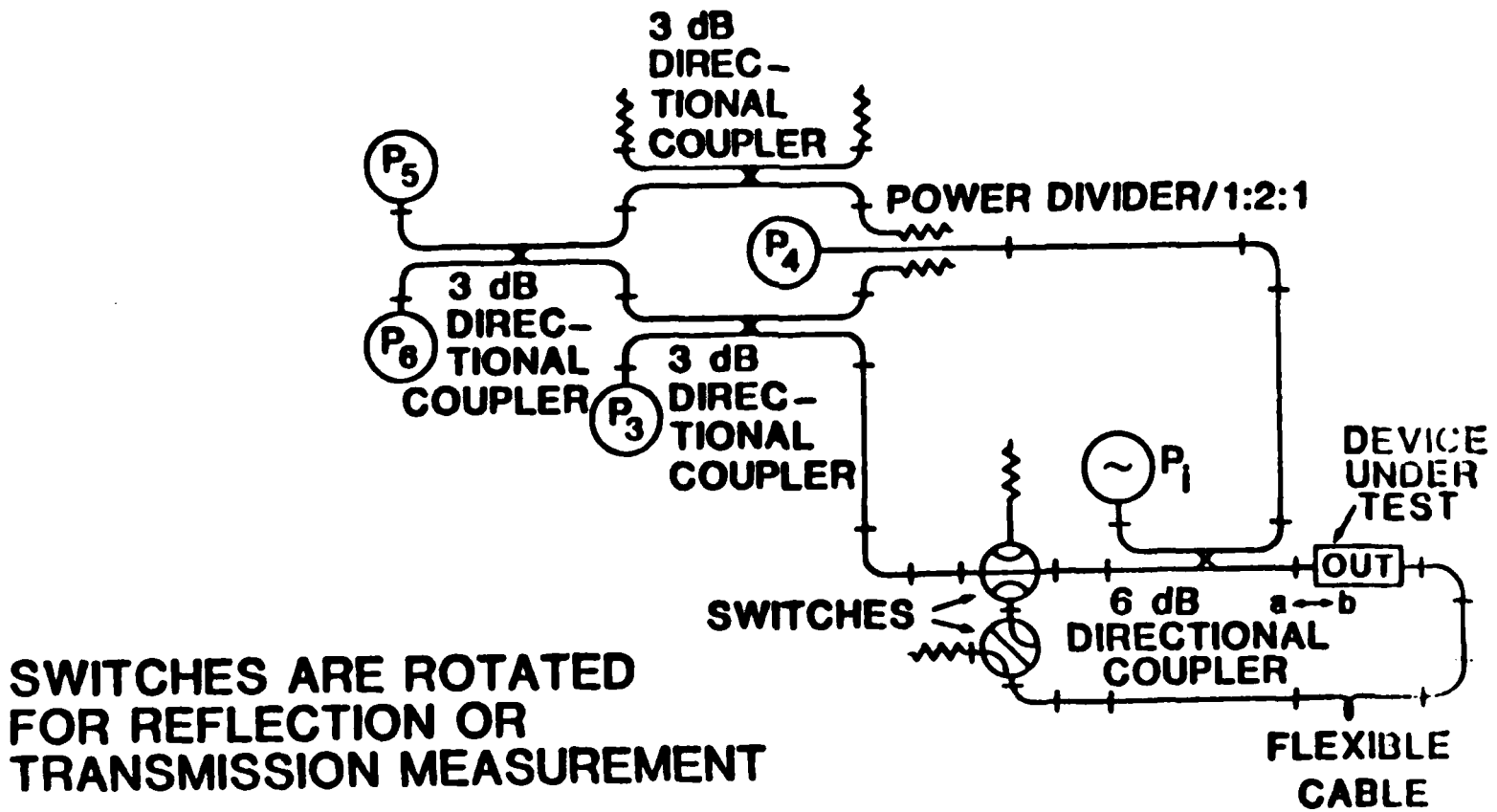

Figure 10. Six-Port Network Analyzer

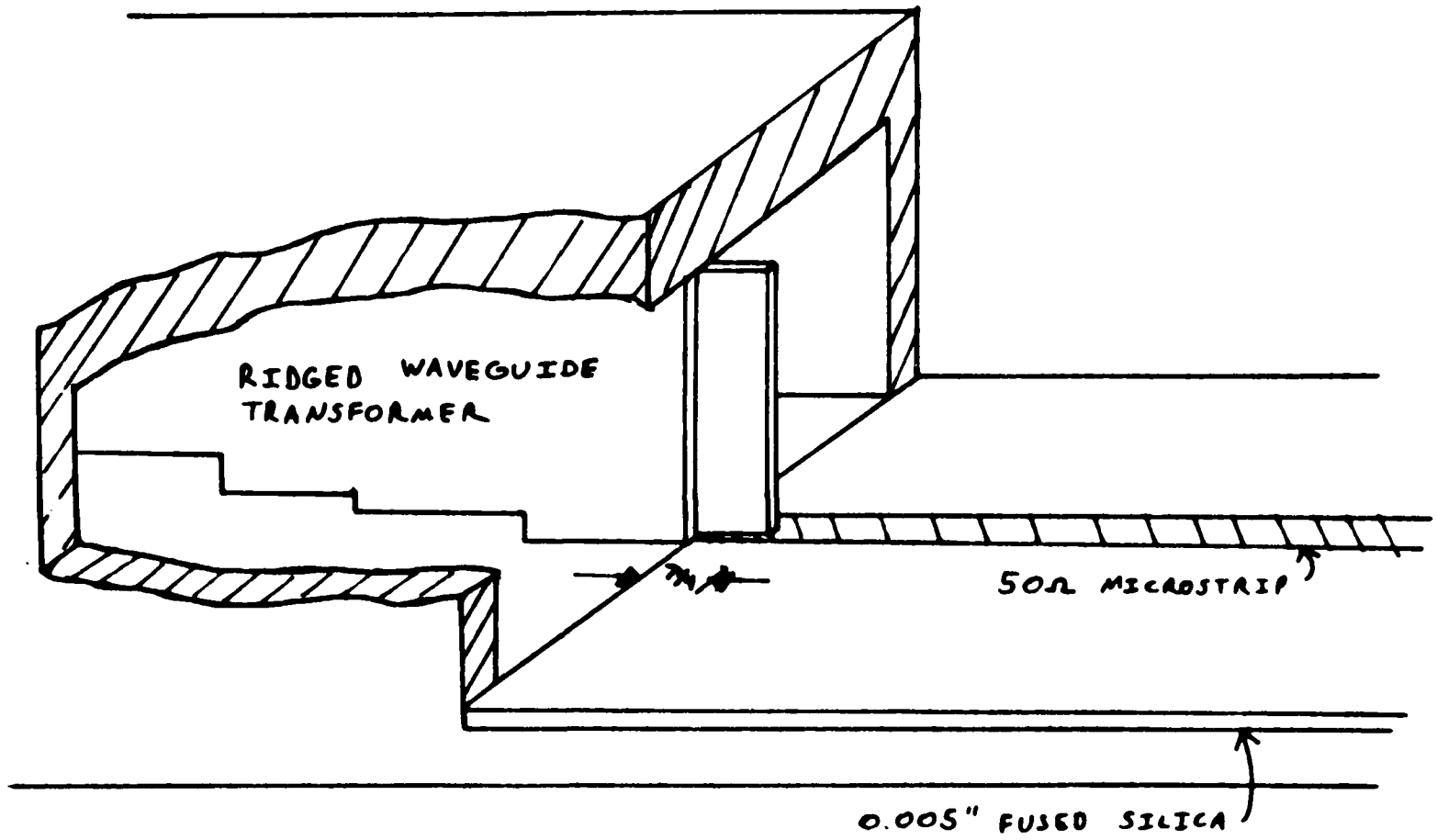

Figure 11. Waveguide to Microstrip Transition

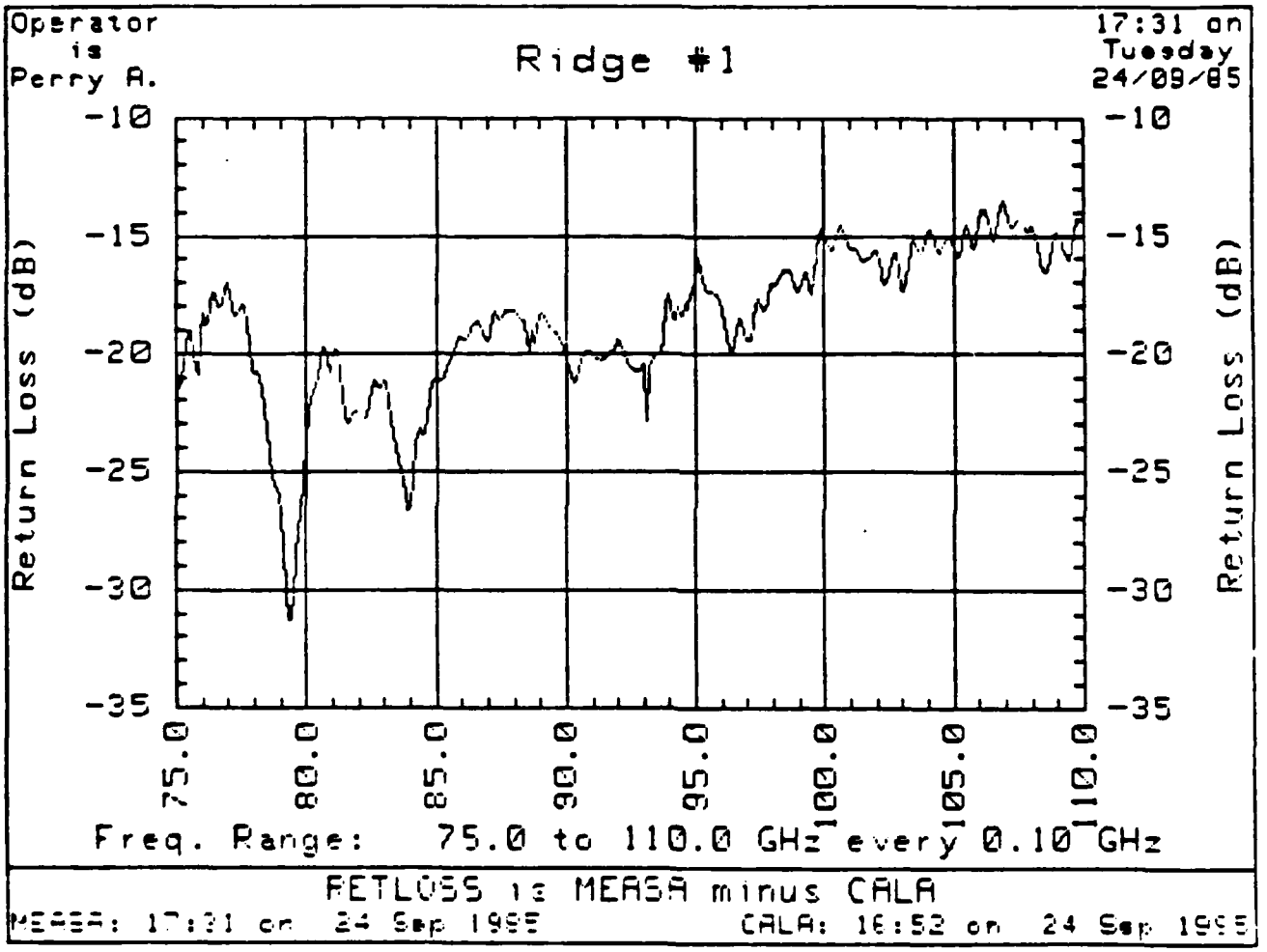

Figure 12. Return Loss of the Transition

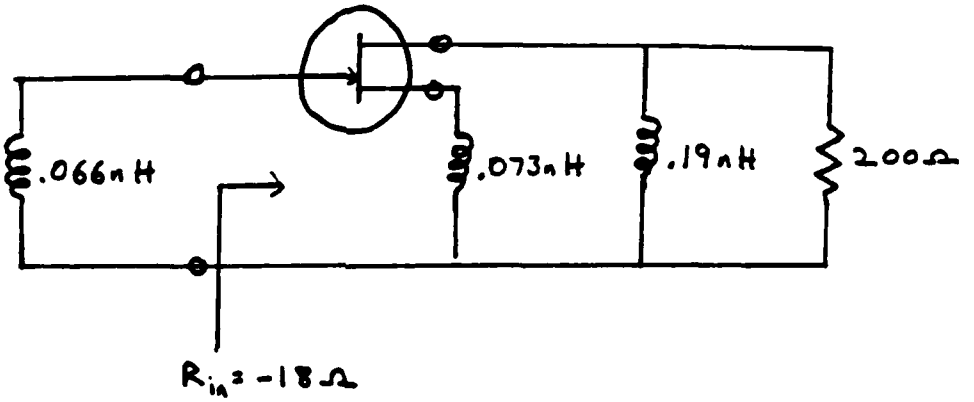

Figure 13. HEMT Oscillator Schematic

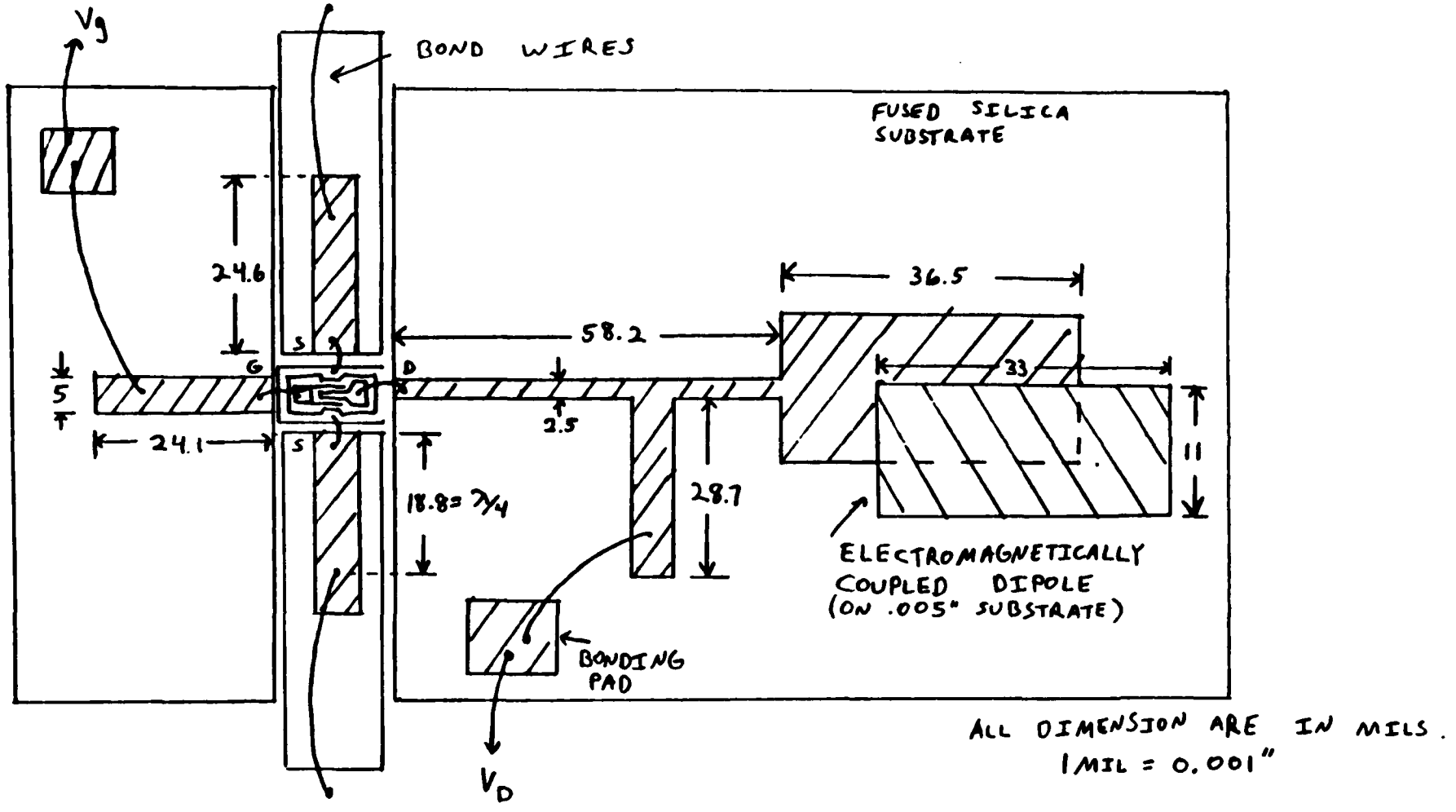

Figure 14. Oscillator Circuit Realization

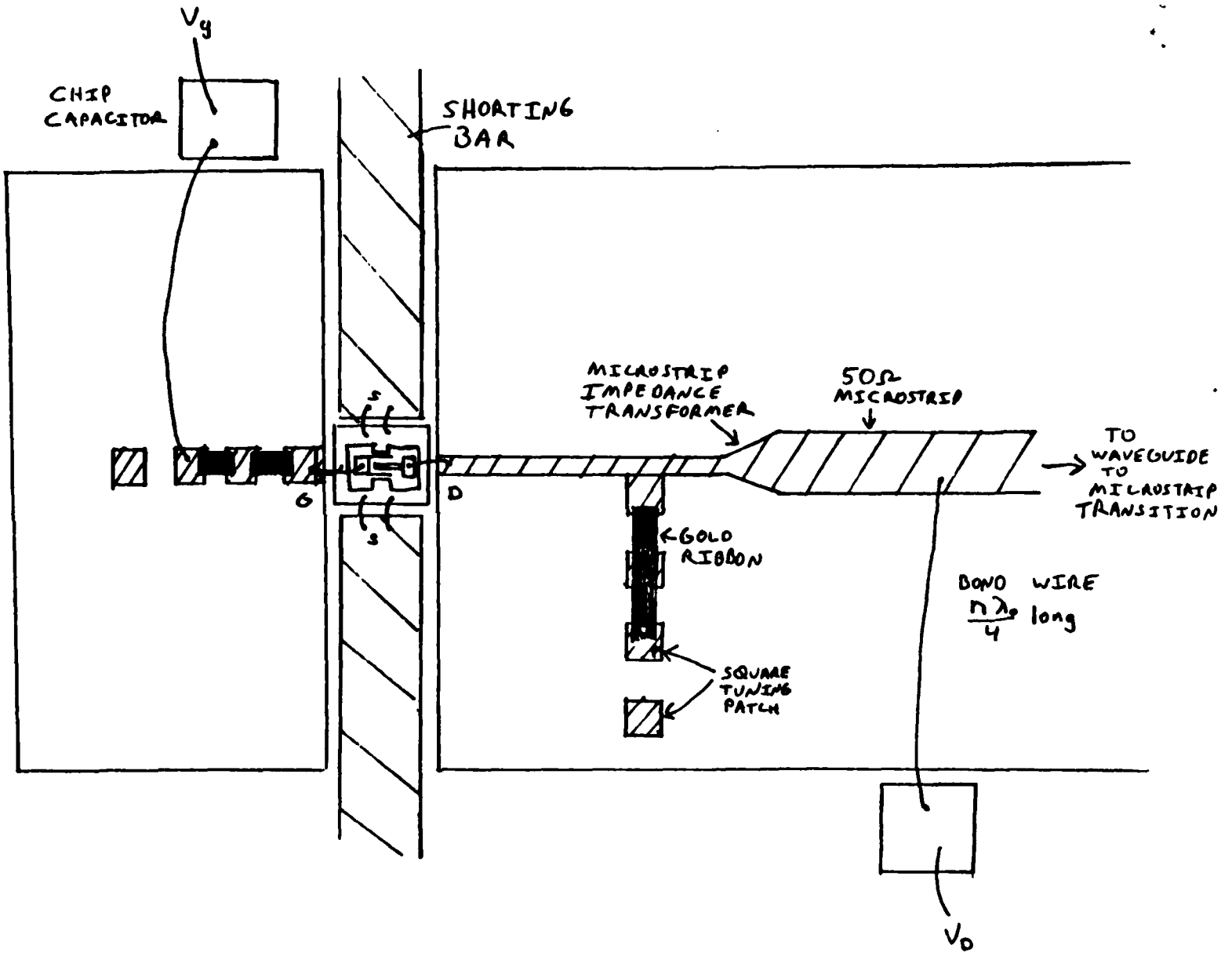

Figure 15. Improved Oscillator Design

END

7-87

DTIC